1. INTRODUCTION

Multiport minichannel and microchannel aluminium tubes are becoming more popular as components in heat exchangers. These heat exchangers are used in various industrial applications and are produced in large quantities with many different geometries and lengths and, therefore, they are relatively inexpensive. The ability to produce tubes with external or internal fins and with smaller wall thicknesses allows higher heat transfer area per unit volume of a tube. Therefore, mini- and microchannel tubes are ideal for use in compact and light weight heat exchangers. The use of minichannel or microchannel heat exchangers in refrigeration equipment, offers the possibility of low refrigerant charges as well as high heat transfer and compact designs. The estimation of heat transfer in condensation and boiling in minichannels is more difficult than that for single-phase flow. However, accurately estimated single-phase heat transfer coefficients will help to determine two-phase heat transfer coefficients.

The distinction between minichannels or microchannels is given by Kandlikar, defines tubes with channel diameters between 0.01 and 0.2mm as microchannels, channel diameters between 0.2 and 3 mm as minichannels, and channel diameters greater than 3mmas conventional channels. However, others prefer a diameter of 1mm as the demarcation between microchannels and minichannels.

They noted that the Reynolds numbers at the exit of the channels were about two to three times higher than that at the inlet in laminar flow. The reason for this difference was given as the rapid change of fluid properties along the channel length. According to their report, fully developed turbulent flow starts in the Reynolds number range of 1000– 1500 and the laminar-to-turbulent flow transition occurs in the Reynolds number range of 300–800.

2. HEAT EXCHANGERS

Heat exchangers are device that facilitate the exchanger of heat between two fluids that are at different temperatures while keeping them from mixing with each other. Heat exchanger are commonly used in practise in a wide range of application, from heating & air conditioning systems in a household, to chemical processing & power production in large plants.

2.1. OBJECTIVES:

1. Recognize numerous types of heat exchangers, and classify them.
2. Perform a general energy analysis on heat exchangers.
3. Know the primary consideration in the selection of heat exchanger.
4. Develop an awareness of fouling on surfaces, and determine the overall heat transfer coefficient for heat exchanger.

2.2. TYPES OF HEAT EXCHANGER:

Heat exchanger may be classified into several types. One classification is according to the fluid flow arrangement or the relative direction of the hot and cold fluids Two types of flow arrangement are possible in a double-pipe heat exchanger are:

1. Parallel Flow
2. Counter Flow
3. Single Pass
4. Cross Flow

If both the fluids moves in same direction, the arrangement is called parallel flow heat exchanger. If the fluids moves in parallel but in opposite directions, the arrangement is called counter flow heat exchanger. In double pipe heat exchanger, either the hot or cold fluid occupies the annuglar space and the other fluids moves through the inner pipe. Since both fluid streams transverse the exchanger only once, this arrangement is called a single pass heat exchanger. Another flow configuration is one in which the fluids move at right angles to each other through the heat exchanger. This type of arrangement is called cross flow type heat exchanger. Cross floe type heat exchanger is used in air heating application. Heat exchanger is used in air conditioning applications.

3. MINICHANNEL HEAT EXCHANGER

3.1 Construction

The heat exchanger was made using 30 multiport extruded aluminium tubes. A picture of a tube cross-section is shown in Fig. 3.1.

Fig 3.1 Tube cross section

Each tube consisted of six channels. The four middle channels were equal in size: 1 mm in height and 2.65mm in width. The two channels at the edges were 1 mm in height with a width of 1.45mm plus a semi-circular part with a radius of 0.5 mm. The wall thickness of the tube was 0.5 mm. The cross-sectional area and wetted perimeter of a tube were taken as the total of all six channels when calculating the hydraulic diameter. The tubes, each with the length 661mm, active heat transfer length, were arranged in two rows and held in place by 31 equally spaced 1-mm thick aluminium baffle plates. The ends of the tubes were fixed to two 5-mm thick aluminium end plates. The tube bundle was placed inside a shell made from four aluminium plates. The whole unit was brazed together at the connecting points. Each baffle plate was joined to three shell plates and a 4.5 mm gap was left to the fourth plate. Ports were added at the ends of the heat exchanger to serve as inlet and outlet ports for the shell-side fluid. Pyramid shaped end caps were attached to the two end plates, acting as inlet and outlet distributors for the tube-side fluid.

The active heat transfer areas on the tube-side and shell-side of the heat exchanger were approximately 0.78m^2 and 0.82m^2, respectively. Total length of the heat exchanger was approximately 700 mm.

A picture of the complete heat exchanger is shown in Fig 3.2

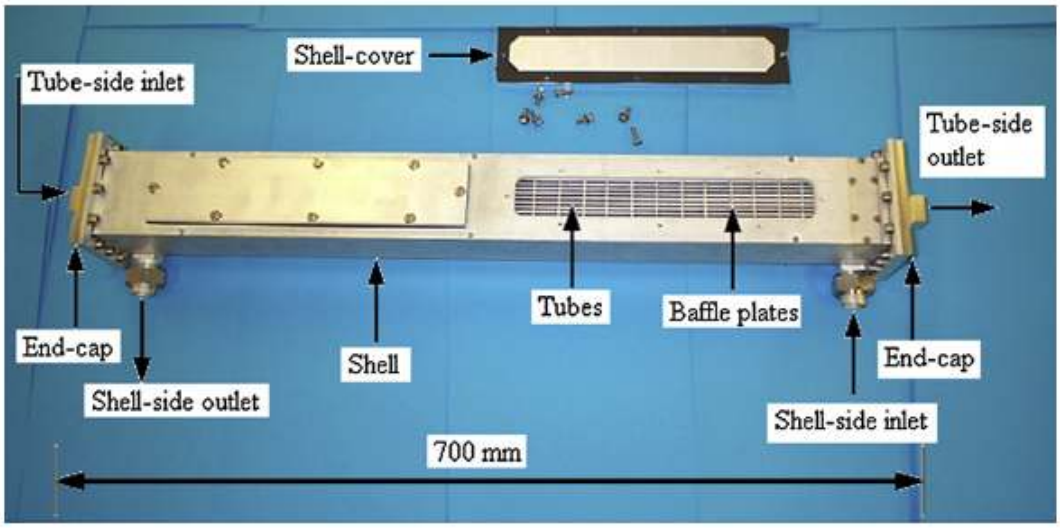

Fig 3.2 Picture of Heat Exchanger

3.2 Working

Working of mini channel heat exchanger based on the principle of counter flow heat exchanger. Warm water enters the tubes from one end-cap, passes through the tubes and leaves through the other end-cap. Cold water enters the shell-side of the heat exchanger through the provided inlet port on the shell, flows through the slots between two adjacent tubes and two adjacent baffle plates, traces a serpentine path due to the baffle plates and exits through the other port.

A section of the shell-side of the tube bundle is shown in Fig.3.3

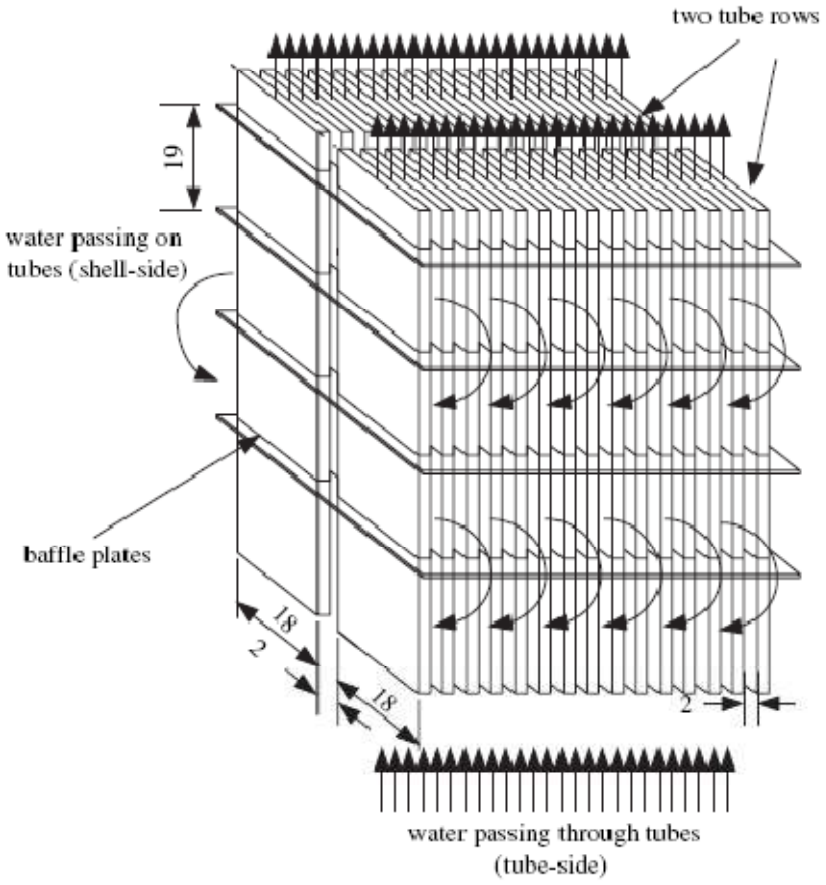

Fig. 3.3 Section of the shell-side of the tube bundle

4. THE WILSON PLOT METHOD

The ‘‘Wilson plot method’’ is applied to determine heat transfer coefficients on the two sides of a heat exchanger from measurements of the overall heat transfer coefficients at different flow velocities on one side and constant conditions on the other side. The overall temperature difference between the two fluids,warm water and cold water in the heat exchanger is written as the sum of the fluid-to-wall temperature differences on each side and the temperature difference across the wall.

The logarithmic mean temperature difference (LMTD) is used as the temperature difference between the two fluids. This implies the assumptions of counter-current flow and uniform heat transfer coefficients along the flow path. The heat transfer rate is calculated as,

$$Q = m.Cp.(\Delta T)\text{along flow path}$$

Correlations for average Nusselt number are typically expressed in the form,

$$Nu = C_0 \, Re^n \, Pr^{0.4} \, (\mu/\mu_s)^{0.14}$$

Where,

$$Nu = (\alpha d_h)/k \; , \; Re = (\square v d_h)/\mu, \; Pr = (\mu C_p)/k, \; C_o = \text{constant}$$

The value of the exponent n is expected to be about 0.8 for turbulent flow in tubes. However, the best value can be found from the data by varying n until the best linear fit to the data is obtained.

5. EXPERIMENTAL SETUP AND PROCEDURE

5.1 Setup

A schematic diagram of the test facility is shown in Fig.4.1. The minichannel aluminium heat exchanger was mounted vertically. Warm water entered the heat exchanger tubes through the lower end-cap and left through the upper end-cap. Cold water entered the shell-side of the heat exchanger through the upper shell port and left through the lower shell port.

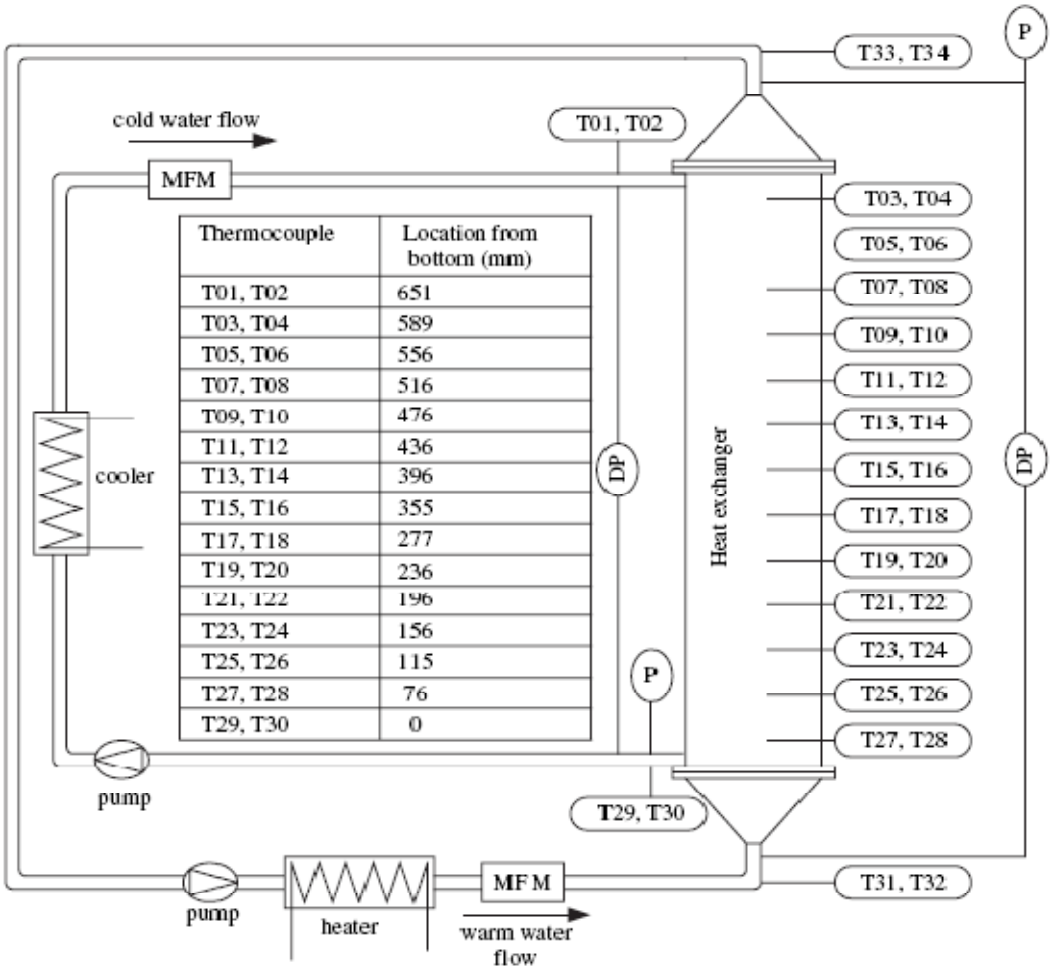

Thermocouple	Location from bottom (mm)
T01, T02	651
T03, T04	589
T05, T06	556
T07, T08	516
T09, T10	476
T11, T12	436
T13, T14	396
T15, T16	355
T17, T18	277
T19, T20	236
T21, T22	196
T23, T24	156
T25, T26	115
T27, T28	76
T29, T30	0

Fig.5.1 Experimental setup

Two magnetic flow meters (MFM) were mounted on the inlet side for both fluids. Warm water inlet and outlet temperatures were measured by four thermocouples, two at each location. These thermocouples were installed in the tube-side fluid distribution lines connected to the heat exchanger. These thermocouples were installed in the tube-side fluid distribution lines connected to the heat exchanger. The temperature of the cold water flow was measured by 30 thermocouples, at the inlet, at various locations along the shell and at the outlet, with two thermocouples at each location (lengths from the bottom of the heat exchanger are shown in Fig. 4.1). Pressure data for the tube and shell-side were acquired from absolute pressure transducers mounted on the water outlet lines and differential pressure transducers connected between the inlet and outlet water lines.

5.2 Procedure

Considerably, big ice-bath was prepared in a well insulated thermos flask. Then all the thermocouples were placed at a same height just below the ice level of the icebath. The temperature readings from the thermocouples were recorded during a long period and observed that they stabilized around 0^0c. The temperature readings of the thermocouples were taken during a 15-min period. Assuming the temperature of the ice-bath as 0^0 C, the average deviation of each of the thermocouple was calculated. Then the

Computer program was adjusted by adding and subtracting the deviations for each of the thermocouples. After adjusting the computer program, further temperature measurements of the ice-bath was taken and the maximum error of each of the thermocouple was found ±0.04. The pressure transducers were calibrated against standard calibrating equipment and uncertainties were ±0.02%. Due to limitations in pump capacities, there were constraints on the test facility flow rates. The maximum flow rate of the cold water under the test conditions was 37 $lmin^{-1}$. For that flow rate, Re=4800 at 30^0 C. The maximum flow rate of warm water was 82 $lmin^{-1}$, producing Re=6000 at 30^0 C. These Reynolds numbers indicate that both flows were in the laminar (Re < 2300) to transition regions (2300 < Re < 10,000), as defined for large diameter channels. For the investigation of the heat transfer on the tube-side, the cold

water flow rate (shell-side) was maintained at its maximum value (37 $lmin^{-1}$) during the test period.

At the first test point, the warm water (tube-side) flow rate was also adjusted to its maximum value (82 $lmin^{-1}$). At steady state, temperatures, pressures, and flow rates were recorded every 5 s for approximately 5 min. The warm water flow rate was decreased incrementally while the cold water flow rate was fixed. At each increment, measurements were recorded at stable conditions. For the investigation of the influence of flow rate on the shell-side heat transfer, experiments were conducted with the warm water flow rate fixed at 75 $lmin^{-1}$ while the cold water flow rate was incremented downward step by step.

Using the least squares method, the best fit of the shell-side temperature data as a function of distance from the entrance was determined. Then the temperatures throughout the heat exchanger were re-estimated from the curve fit equation. Temperatures at the corresponding locations on the tube-side were calculated from the heat balance between the two fluids. The Prandtl number range was $5.15 < Pr < 5.30$ for all tests.

6. CORRELATIONS

6.1 Laminar Flow Region

The experimental data were compared to the heat transfer correlations presented in Table 1, valid for laminar flow in the entry region and fully developed region.

The hydrodynamic entry length for laminar flow in a tube is obtained from the expression,

$$(X_{fd,h}) / d_h = 0.05\ Re$$

The thermal entry length for laminar flow in a tube is obtained from,

$$(X_{fd,t}) / d_h = 0.05\ Re.Pr$$

These two eqs. indicate that hydrodynamically fully developed conditions should be reached more rapidly than thermally fully developed conditions in cases of $Pr > 1$.

Table 1 – Correlations from the literature for the laminar flow regime

References	Correlations
Kays (1955) and Hausen (1943) Thermal entry length	$\overline{Nu} = 3.66 + \dfrac{0.0668(d_h/L)Re\,Pr}{1 + 0.04[(d_h/L)Re\,Pr]^{1/3}}$
Constant wall temperature Circular tubes	$Pr \gg 1$ or hydrodynamic developed flow at tube inlet
Sider and Tate (1936) Combined entry length	$\overline{Nu} = 1.86\left(\dfrac{Re\,Pr}{L/d_h}\right)^{1/3}\left(\dfrac{\mu_w}{\mu_s}\right)^{0.14}$
	$0.48 < Pr < 1670$ and $0.0044 < \dfrac{\mu_w}{\mu_s} < 9.75$
Srinivas et al. (2001)	$\overline{Nu} = \left(Nu_{lam}^{10} + \left\{\dfrac{\exp[(360 - Re)/925]}{Nu_{lam}^2} + \dfrac{1}{Nu_{turb}^2}\right\}^{-5}\right)^{0.1}$
	$Nu_{lam} = \left(Nu_{fd}^3 + \left\{\dfrac{0.468(d_h/L)Re\,Pr}{\left\{1 + 0.165[(d_h/L)Re\,Pr]^{2/3}\right\}}\right\}^3\right)^{1/3}\left(\dfrac{\mu_w}{\mu_s}\right)^{0.25}$
	$Nu_{fd} = 8.235(1 - 2.0421Z + 3.0853Z^2 - 2.4765Z^3 + 1.0578Z^4 - 0.1861Z^5)$
	$Z = \dfrac{\min(H,W)}{\max(H,W)}$
	$Nu_{turb} = 0.012Re^{0.85}Pr^{0.4}\left[1 + \left(\dfrac{d_h}{L}\right)^{2/3}\right]\left(\dfrac{\mu_w}{\mu_s}\right)^{0.25}$
	$0.243 < \dfrac{\mu_w}{\mu_s} < 0.630$; $118 < Re < 10671$; $0.243 < Pr < 16.20$
Hartnett and Kostic (1989) Rectangular tubes Fully developed flow	$Nu = 8.235(1 - 2.0421Z + 3.0853Z^2 - 2.4753Z^3 + 1.0578Z^4 - 0.1861Z^5)$
Shah and London (1978) Thermally developing Constant wall heat flux	$Nu = \begin{cases} 1.953\left(Re\,Pr\dfrac{d_h}{L}\right)^{1/3}; & \left(Re\,Pr\dfrac{d_h}{L}\right) \geq 33.3 \\ 4.364 + 0.0722\left(Re\,Pr\dfrac{d_h}{L}\right); & \left(Re\,Pr\dfrac{d_h}{L}\right) \leq 33.3 \end{cases}$
Peng and Peterson (1996) Rectangular tubes Micrcchannels Fully developed	$Nu = 0.1165\left(\dfrac{d_h}{W_c}\right)^{0.81}(Z)^{-0.79}Re^{0.62}Pr^{1/3}$; $Z = \dfrac{\min(H,W)}{\max(H,W)}$; $Re < 2,200$ where W_c = centre-to-centre distance between two channels
Choi et al. (1991)	$Nu = 0.000972Re^{1.17}Pr^{1/3}$; $Re < 2000$

6.2. Transition Flow Region (2300 < Re < 10,000)

Correlations by Gnielinski (1976), Dittus and Boelter (1930) and Kakac et al. (1987) as well as other correlations presented in Table 2, which are recommended for the turbulent flow region, were compared to the experimental data.

7. RESULTS AND DISCUSSION

7.1. Heat Transfer Coefficient on Tube-Side (Warm Water) in The Transition Flow

Range, 2300 < Re < 6000

The inverse of the overall heat transfer coefficient (1/U) was plotted versus the inverse of the warm water flow rate to the power of n (1/ V^n_{warm}).

Table 2 – Correlations from the literature for the transition and turbulent flow ranges

Reference	Correlations
Gnielinski (1976) Circular tubes	$Nu = \frac{(f/8)(Re-1000)Pr}{1+12.7(f/8)^{1/2}(Pr^{2/3}-1)}$; $f = (0.790\ln Re - 1.64)^{-2}$; $3000 < Re < 5{,}000{,}000$; $0.5 < Pr < 2000$
Dittus and Boelter (1930)	$Nu = 0.023Re^{0.8}Pr^{0.3}$; $Re > 10{,}000$; $0.7 < Pr < 160$
Kakac et al. (1987) $2300 < Re < 10{,}000$	$Nu = 0.116\left(Re^{2/3}-125\right)Pr^{1/3}\left(1+\left(\frac{d_h}{L}\right)^{2/3}\right)\left(\frac{\mu}{\mu_w}\right)^{0.14}$
Choi et al. (1991) Circular microchannels	$Nu = 3.82\times10^{-6}Re^{1.96}Pr^{1/3}$; $2500 < Re < 20{,}000$
Peng and Peterson (1996)	$Nu = 0.072\left(\frac{d_h}{W_c}\right)^{1.15}\left[1-2.421(Z-0.5)^2\right]Re^{0.8}Pr^{1/3}$
Rectangular microchannels	where $W_c = 3.15$ mm (distance between two channels), $Z = \frac{\min(H,W)}{\max(H,W)} = \frac{1}{2.65}$
Debray et al. (2001) Rectangular microchannels	$Nu = 0.0593Re^{3/4}Pr^{1/3}$; $4000 < Re < 10{,}000$
Wu and Little (1983) Microchannels	$Nu = 0.00222Re^{1.09}Pr^{0.4}$; $3000 < Re < 20{,}000$
Yu et al. (1995) Microchannels	$Nu = 0.007Re^{1.2}Pr^{0.2}$; $6000 < Re < 20{,}000$

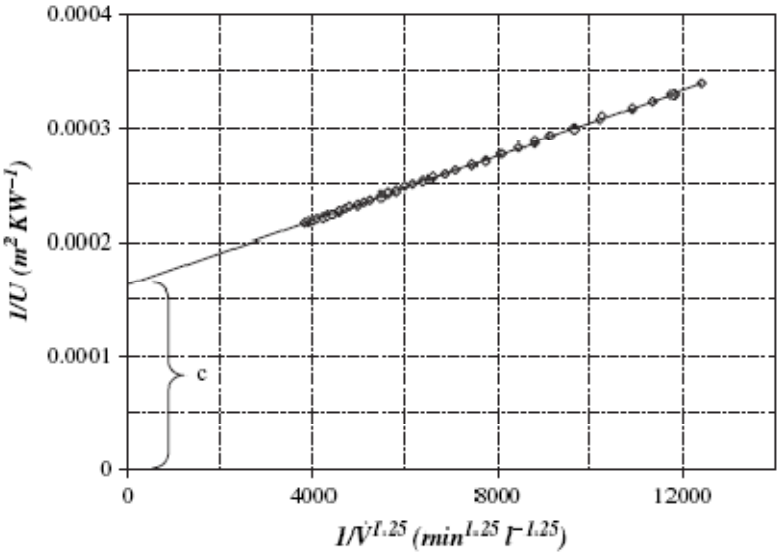

Fig.7.1.1 Graph of (1/U) vs (1/ V^n_{warm}).

With the exponent n = 1.25, the minimum variance was obtained and all the data in the Reynolds number range of 2300–6000 followed a straight line, as shown in Fig. 6.1 However, the data for Re < 2300 did not follow the straight line. Therefore, the value n = 1.25 was chosen as the Reynolds exponent for the tube-side of the heat exchanger for 2300< Re < 6000.

The experimental and predicted Nusselt numbers were area averaged and are shown as a function of Re in Fig.7.1.2. The difference between predicted and experimental average Nu, expressed as a percentage with the experimental average Nu as the base, is given in Table 3.

Table 3 – Maximum and minimum difference between predicted and experimental average Nusselt numbers for 2300 < Re < 6000

Correlation	Minimum diff. (%)	Maximum diff. (%)
Yu et al. (1995)	620	657
Choi et al. (1991)	79	265
Debray et al. (2001)	55	147
Wu and Little (1983)	23	42
Dittus and Boelter (1930)	3	57
Gnielinski (1976)	−5	6
Kakac et al. (1987)	−4	−31
Srinivas et al. (2001)	−12	−19
Peng and Peterson (1996)	−30	−54

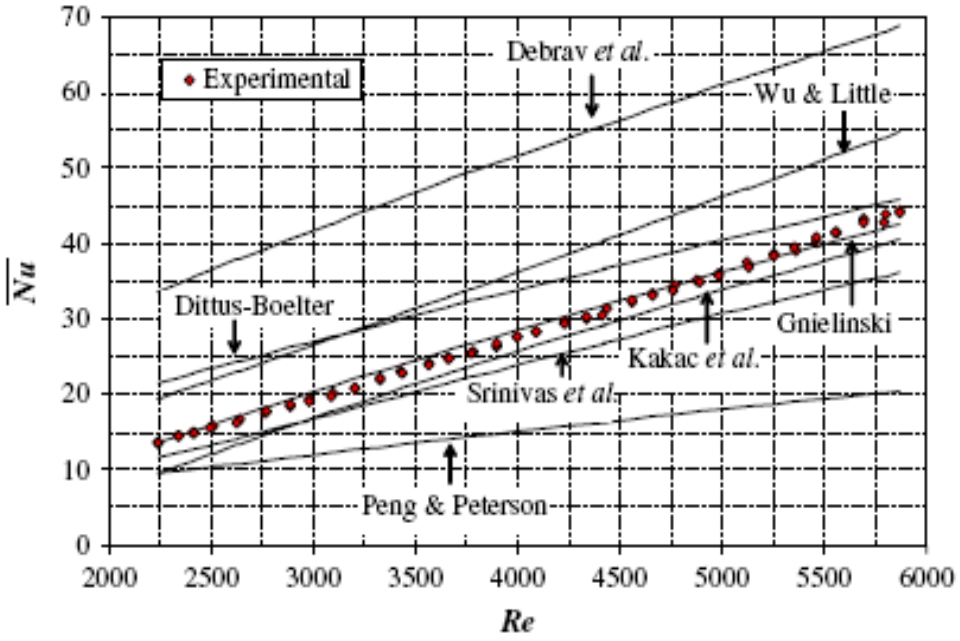

Fig.7.1.2 Comparison of experimental and predicted average Nu

The data in Fig.7.1.2 and Table 3 indicate that the experimentally determined average Nusselt numbers are in excellent agreement with the average Nusselt numbers predicted by the correlation of Gnielinski (1976). The correlations presented by Kakac et al. (1987) and Srinivas et al. (2001) slightly under predict the average Nusselt numbers. The correlation presented by Peng and Peterson (1996) for microchannels predicts much lower average Nusselt numbers. The Dittus and Boelter (1930) correlation, originally suggested to be used for Re > 10,000, over predicts the average Nusselt number at the lower end of the tested Re range while at higher Re (6000), the agreement with the experimental average Nusselt numbers was quite good.

7.2. Heat Transfer Coefficients on The Tube-Side (Warm Water) in The Laminar Range 170 < Re < 2300

The variation in Nu with Re for laminar flow from the tests and from the correlations listed in Table 1 is shown in Fig.6.2.3. Note that the average Nu trend changes at approximately Re = 1250. The average Prandtl numbers of the above tests were in the range 5.30–6.60.

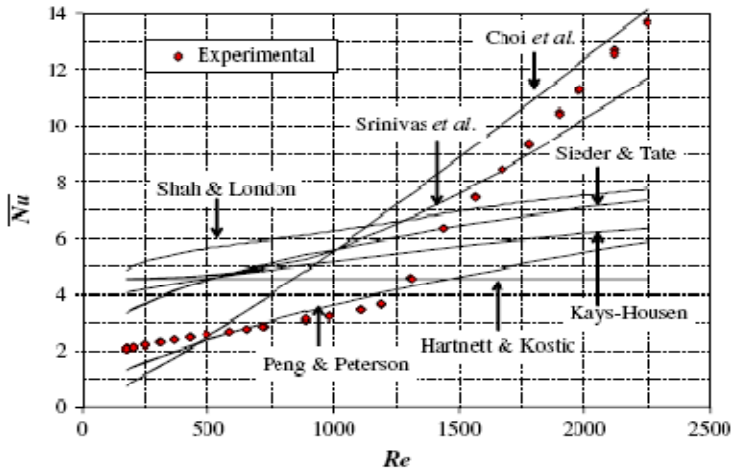

Fig.7.2 The variation in Nu with Re

7.3. Heat Transfer Coefficient on The Shell-Side

The experimental shell-side average Nusselt number variation with the average Reynolds number is shown in Fig.7.3.

The shell-side average Nusselt number is calculated by,

$$Nu = (0.0037Re + 5.532)\ Pr^{0.4}$$

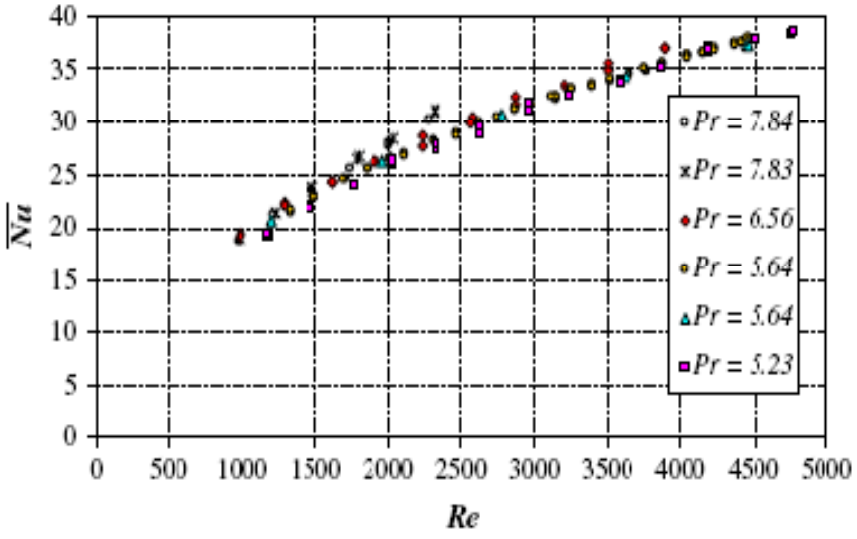

Fig.7.3 Variation of average Nu with Re

8. CONCLUSION

The Wilson plot method was successfully applied to determine the heat transfer coefficients in the laminar and transition flow regimes of a liquid-to-liquid heat exchanger constructed with multiport aluminium minichannel tubes.In the laminar flow range, the tube-side Nusselt numbers were not well correlated by any of the correlations from the data and the experimentally determined Nusselt numbers were considerably lower than expected. The shell-side heat transfer coefficients were also not well predicted from available correlations and the experimental heat transfer coefficients were higher than expected.

9. REFERENCES

1. A minichannel aluminium tube heat exchanger – Part I: Evaluation of single-phase heat transfer coefficients by the Wilson plot method; Primal Fernando, Bjorn Palm, Tim Ameel, Per Lundqvist, Eric Granryd.
2. An experimental investigation of single-phase force convection in micro channels. Adams, T.M., Abdel-Khalik, S.I., Jeter, S.M., Qureshi, Z.H., 1998.
3. A minichannel aluminium tube heat exchanger – Part II: Evaporator performance with propane. Primal Fernando, Bjorn Palm, Tim Ameel, Per Lundqvist, Eric Granryd.
4. Heat & Mass Transfer (Third Edition) Prof. Yunus A.Cengel (Emeritus College of Mech.Engg, University Nevada,Reno)